Bull Volcanol (1990) 52:334–354

Bulletin of Volcanology

Phreatomagmatic and phreatic fall and surge deposits from explosions at Kilauea volcano, Hawaii, 1790 A.D.: Keanakakoi Ash Member

Jocelyn McPhie[1]*, George PL Walker[1], and Robert L Christiansen[2]

[1] Hawaii Institute of Geophysics, 2525 Correa Road, Honolulu, HI96822, USA
[2] US Geological Survey, 345 Middlefield Road, Menlo Park, CA94025, USA

Received July 28, 1989/Accepted November 9, 1989

Abstract. In or around 1790 A.D. an explosive eruption took place in the summit caldera of Kilauea shield volcano. A group of Hawaiian warriors close to the caldera at the time were killed by the effects of the explosions. The stratigraphy of pyroclastic deposits surrounding Kilauea (i.e., the Keanakakoi Ash Member) suggests that the explosions referred to in the historic record were the culmination of a prolonged hydrovolcanic eruption consisting of three main phases. The first phase was phreatomagmatic and generated well-bedded, fine fallout ash rich in glassy, variably vesiculated, juvenile magmatic and dense, lithic pyroclasts. The ash was mainly dispersed to the southwest of the caldera by the northeasterly trade winds. The second phase produced a Strombolian-style scoria fall deposit followed by phreatomagmatic ash similar to that of the first phase, though richer in accretionary lapilli and lithics. The third and culminating phase was phreatic and deposited lithic-rich lapilli and block fall layers, interbedded with cross-bedded surge deposits, and accretionary lapilli-rich, fine ash beds. These final explosions may have been responsible for the deaths of the warriors. The three phases were separated by quiescent spells during which the primary deposits were eroded and transported downwind in dunes migrating southwestward and locally excavated by fluvial runoff close to the rim. The entire hydrovolcanic eruption may have lasted for weeks or perhaps months. At around the same time, lava erupted from Kilauea's East Rift Zone and probably drained magma from the summit storage. The earliest descriptions of Kilauea (30 years after the Keanakakoi eruption) emphasize the great depth of the floor (300–500 m below the rim) and the presence of stepped ledges. It is therefore likely that the Keanakakoi explosions were deepseated within Kilauea, and that the vent rim was substantially lower than the caldera rim. The change from phreatomagmatic to phreatic phases may reflect the progressive degassing and cooling of the magma during deep withdrawal: throughout the phreatomagmatic phases magma vesiculation contributed to the explosive interaction with water by initiating the fragmentation process; thereafter, the principal role of the subsiding magma column was to supply heat for steam production that drove the phreatic explosions of the final phase.

Introduction

Kilauea caldera is surrounded by well-bedded ash and lapilli deposits of the Keanakakoi Ash Member (Easton 1987). The deposits are most conspicuous along the southern and southwestern margin of the caldera where vegetation is sparse and dissecting gullies are numerous. Rim exposures there are 5–12 m thick and comprise more than a dozen separate layers distinguished by an impressive variety in color, grain size, texture, internal bed thickness, and bed forms.

The Keanakakoi Ash Member was deposited prior to the survey of Kilauea by William Ellis in 1823 (Ellis 1827). Ellis established that Kilauea had erupted explosively in 1790, and that part of the member was deposited then. The event figured prominently in local Hawaiian history because it killed a party of warriors travelling near the caldera. However, no accurate and detailed record was made either of the course of the eruption, or of the condition of the caldera and vent(s) within it. It is thus imperative to supplement the scant historical data using the wealth of information incorporated in the deposits. S Powers (1916), Stone (1926), Stearns and Clark (1930), Wentworth (1938), and HA Powers (1948) mapped the distribution and thickness of the deposits, and a very considerable advance was made by Swanson and Christiansen (1973) who recognized base surge deposits within the sequence and pointed out the critical role of magma-water interaction

* *Present address:* Bureau of Mineral Resources, GPO Box 378, Canberra ACT 2601, Australia

Offprint requests to: J McPhie

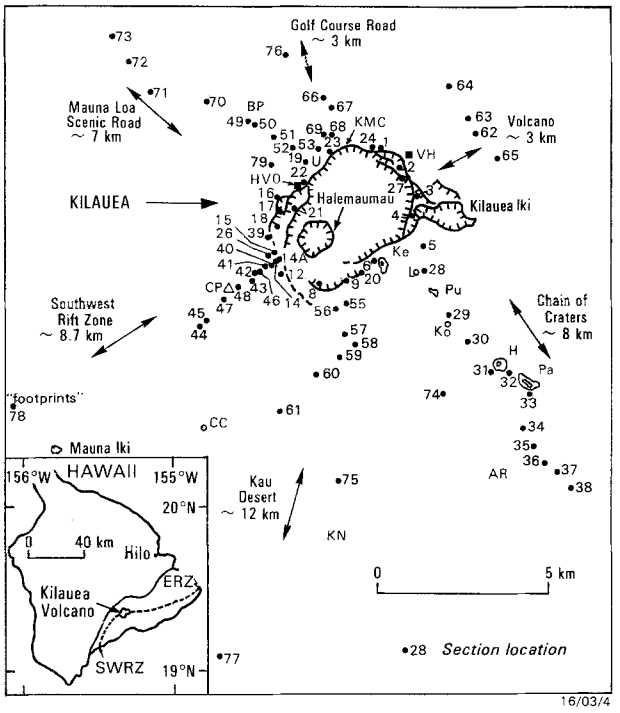

Fig. 1. Location of measured sections through the Keanakakoi Ash Member around and radial to Kilauea caldera, Hawaii. *AR,* Ainahou Ranch; *BP,* Bird Park; *CC,* Cone Crater; *CP,* Cone Peak; *H,* Hiiaka Crater; *HVO,* Hawaii Volcanoes Observatory; *KMC,* Kilauea Military Camp; *Ke,* Keanakakoi Crater; *KN,* Kipuka Nene; *Ko,* Kokoolau Crater; *L,* Lua Manu Crater; *Pa,* Pauahi Crater; *Pu,* Puhimau Crater; *U,* Uwekahuna; *VH,* Volcano House. *Inset: SWRZ,* Southwest Rift Zone; *ERZ,* East Rift Zone

in causing deviations from the typical effusive activity of Kilauea. The internal stratigraphy described by Christiansen (1979) and Decker and Christiansen (1984) formed a basis for their interpretation of the eruption dynamics.

This paper reports the results of additional mapping and detailed stratigraphic analysis of 13 sections around the rim of Kilauea caldera, and another 48 sections distributed along six traverses radiating from the rim (Fig. 1). Correlation of the sections provides a framework for documenting the vertical and lateral variations within the deposits, assessing the importance and duration of time breaks during their accumulation, refining present interpretations of the eruptive style and emplacement processes, and reconstructing the course of events. For the purpose of hazards evaluation, an attempt is also made to identify the coincidence of conditions that will promote explosive eruptions at Kilauea. Investigation of grain size, grain shape, and component proportions is herein limited to qualitative descriptions only.

The Keanakakoi Ash Member

As defined by Easton (1987), the Keanakakoi Ash Member comprises well-bedded ash and lapilli sandwiched between and including lower and upper reticulite pumice layers (Table 1). It rests on prehistoric lava flows or an older ash member (i.e., the Uwekahuna Ash Member, Easton 1987) of the Puna basalt. Close to the southwestern caldera rim there is a thin veneer of lithic debris from the 1924 phreatic eruption of Halemaumau (Jaggar and Finch 1924).

Table 1. Stratigraphic nomenclature, after Easton (1987) and Sharp et al. (1987)

Puna basalt	
Historic lava flows	
Lithic ash and lapilli from Halemaumau (1924)	
Historic lava flows	
Keanakakoi Ash Member	golden pumice, ~1820
	Keanakakoi ash, 1790
	basal reticulite, pre-1790
Prehistoric lava flows & the Uwekahuna Ash Member	

The upper reticulite layer was informally named the "golden pumice" by Sharp et al. (1987), who considered it to be the composite of perhaps one or two years of lava fountaining within the caldera during the period 1790–1823, most probably about 1820 A.D. The basal reticulite is widely distributed, except around the southern to southeastern sectors, and is separated from the rest of the member by an erosion surface. Like the golden pumice, the basal reticulite may also be a composite record of many summit fire-fountain eruptions.

The time span represented by the deposits between the basal reticulite and the golden pumice is in dispute, largely arising from differing interpretations of the Hawaiian eyewitness accounts and of the significance of internal disconformities. Several early authors (Hitchcock 1909; S Powers 1916; Stone 1926; Stearns and Clark 1930; Wentworth 1938; Finch 1947; HA Powers 1948) attribute only the upper, lithic-rich beds immediately below the golden pumice to the 1790 explosions. More recent authors (Christiansen 1979; Malin et al. 1983; Decker and Christiansen 1984; Easton 1987) propose that all of the member between the two reticulite layers is the product of a single, essentially continuous eruptive phase lasting several days to a few weeks.

We find merit and error in each interpretation. The explosions reported to have occurred in 1790 are readily correlated with the upper, lithic-rich beds of the member. However, this portion is separated from the remainder by a widespread disconformity, and there are at least two older erosion surfaces and reworked intervals (in part described by Malin et al. 1983). Furthermore, features of the deposits reflect quite marked changes of eruptive style and dispersal direction during their accumulation. It is likely therefore that a more prolonged period was involved (several months?) than envisaged by modern interpretations. At the same time, the new data are consistent with the view that the entire sequence between the reticulite layers is genetically related to a coherent, though punctuated, eruption episode clearly different from the norm for Kilauea. It is proposed herein that the Hawaiians described only the

culminating phase of this eruption, lasting little more than a few days during 1790, to Ellis (1827) and Dibble (1843).

The Keanakakoi Ash Member thus includes at least 3 parts, the middle part being the principal concern of the following text wherein it is referred to as "Keanakakoi ash".

Keanakakoi ash

Keanakakoi ash comprises 16 main layers distinguished by contrasts in color, grain size, composition, depositional structures, and coherence, and commonly separated by sharp bedding planes (Fig. 2, Table 2). In thick proximal sections, each layer is internally bedded and could be subdivided further, though no attempt was made to map these fine-scale variations. No section includes every one of the 16 layers, although the thickest sections along the southern rim lack only a few of the minor layers. The characteristics of each layer summarized on Fig. 2 and Table 2 are drawn mainly from these thick exposures.

Notwithstanding the considerable complexity layer to layer vertically through Keanakakoi ash, most sections can be readily subdivided into three parts: a lower, well-bedded, vitric ash division, and an upper, lithic-rich block and ash division, separated by a heterogeneous division of ash and lapilli variously showing affinities with either or both of the lower or upper divisions. These divisions match the Lower Mixed Unit, Upper Lithic Unit, and Intermediate Vitric Unit, respectively, of Malin et al. (1983).

The bulk deposit volume of the Keanakakoi ash is approximately 0.108 km^3, calculated by summing the area-times-thickness values of successive isopachs. The lower division accounts for about 40% of this total; the middle and upper divisions constitute some 30% each.

The lower, well-bedded, vitric ash division

The four layers included in this division (1, 2, 3, 4), are characterized by the following:

a) olive-brown and pale-yellow color;

b) relatively fine grain size – the predominant grade is ash, ranging to fine lapilli ($\leqslant$ 16 mm) with scattered coarser lapilli of low-density, basaltic pumice;

c) dominance of juvenile pyroclasts comprising olive-yellow, sideromelane and shiny, black glass (tachylite?) in the ash grade, and black to dark-gray scoria and highly vesicular, yellow-olive, partly palagonitized pumice in the fine lapilli grade. The latter grade also contains significant amounts of nonjuvenile accessory clasts, principally dense basaltic lithics, and crystal fragments (olivine and feldspar);

d) relatively good sorting of individual laminae or thin beds. In detail, the coarser grade, thin beds are locally poorly size sorted, including smaller, higher-density lithics and larger, lower-density pumice;

e) well-developed bedding – planar, even, continuous

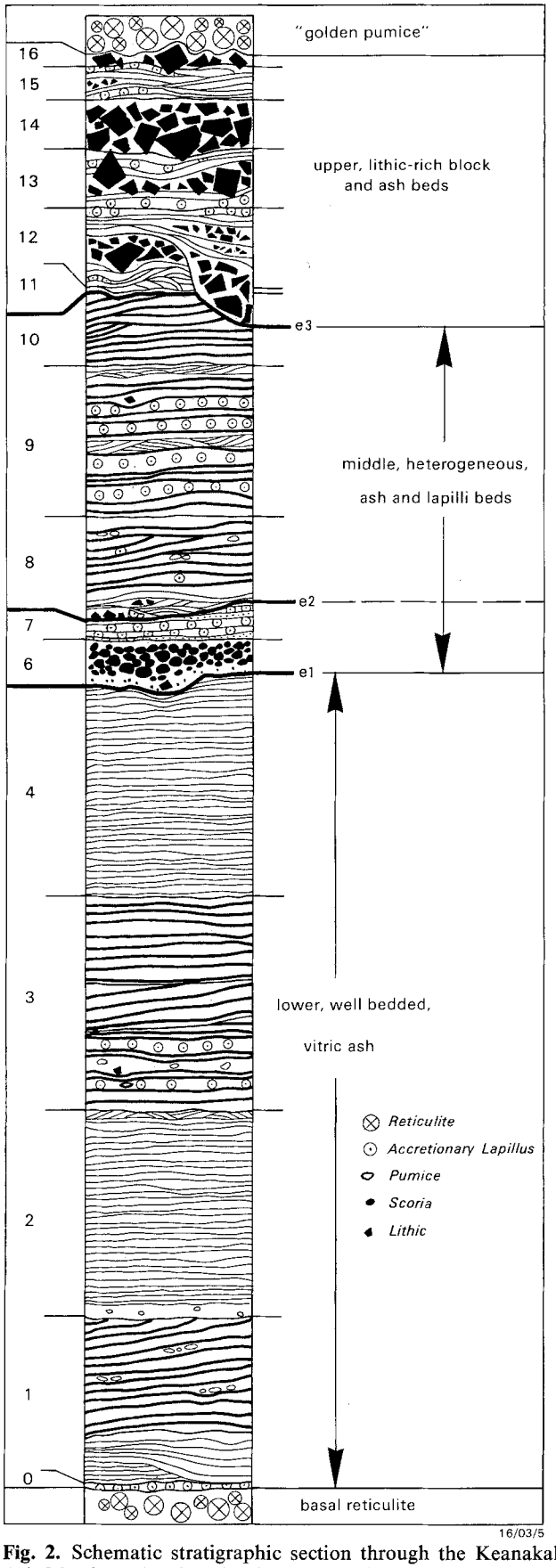

Fig. 2. Schematic stratigraphic section through the Keanakakoi Ash Member, showing the three main divisions and component layers 0 to 16, between basal and upper reticulite pumice deposits. e1, e2, and e3 are erosion surfaces. The lower and middle divisions largely comprise fallout deposits; the upper division also includes base surge deposits

Table 2. Summarized characteristics of the 16 layers comprising the middle part of the Keanakakoi Ash Member (Keanakakoi ash)

Layer	Distribution, T_{max}[a]	Color, fabric, and structure	Grain size[b]	Components[c]	Contacts	Other
Upper, lithic-rich block and ash beds						
16	Close to rim; single clast thickness	Scattered clasts in impact craters	Lapilli and blocks	L	Impact craters deform underlying layers (mainly 15)	Difficult to distinguish from layer 14
15	SW Rift Zone, Golf Course Rd, Volcano? 40 cm (14A)	Purplish-gray, lenticular, and cross-bedded with continuous, even laminae mantling dunes; typically has continuous, thin bed of fine ash at the top	Cross-beds: fine ash to lapilli; Mantling: fine ash	Coarse ash and lapilli: L, C, A; Fine ash: L, C, A?	Gradational lower contact with layer 14; contains embedded blocks and lapilli from layer 16	Distributed in two lobes (N and SW); fine ash laminae rich in accretionary lapilli; surface dunes
14	All rim sections; Chain of Craters Rd, Kau Desert, part of SW Rift Zone; 60 cm (8), 80 cm (21)	Dark-gray-brown; single continuous, even, mantling bed ± diffuse internal bedding defined by grading	Matrix poor, moderately sorted, lapilli and blocks	L	Underlying layers deformed by lapilli and blocks; some blocks deeply embedded into layer 13 and protruding through layer 15	Distinct SE bias in distribution
13	Most rim sections (not the NE); SW Rift Zone, Kau Desert, part of Chain of Craters Rd; 70 cm (14A)	Pinkish-orange; compact, continuous, mantling layer, commonly with 3 subdivisions: c, thin, even ash bed; b, matrix-poor, lensing bed; a, thin, even ash bed with abundant accretionary lapilli	Very poorly sorted blocks to fine ash; c, ash and sparse lapilli; b, blocks and lapilli a, ash and sparse lapilli	Coarse ash and lapilli: L, C, A; Fine ash: L, C, A?	Sharp top; sharp base or else gradation to layer 12 (Chain of Craters Rd); basal ash bed deformed by blocks and lapilli of middle bed	Blocks of middle bed protrude through top ash bed; ± vesicles; ≡ uppermost accretionary lapilli layer at "Footprints"
12	All rim sections; Kau Desert, SW Rift Zone, part of Chain of Craters Rd; ~100 cm (9)	c, purplish, loose to compact, discontinuous, uneven with diffuse internal lenticular- and cross-lamination; thicker in depressions;	c, poorly sorted coarse ash to blocks; ash coating on coarser clasts;	L, C, A	c, lower contact gradational or erosional, lining channels (e.g., section 9);	12b is the most widespread; 12a is more widespread than 12c, both are associated with channels; cannot everywhere identify a, b, c subdivisions; juvenile ash component in 12a is accidental (not primary)
		b, purplish and dark-gray, loose, continuous, uneven bed with diffuse grading and internal bedding;	b, poorly sorted, lapilli to blocks; matrix-poor;	L	b, blocks protrude into 12c and deform bedding of 12a; infilling precut channels (e.g., section 55);	
		a, pinkish to olive-brown, lenticular, uneven bed with diffuse, low-angle cross lamination	a, coarse ash to lapilli	Lapilli: L Coarse ash: mixed	a, gradational to erosional contact with layer 11, erosional contact with lower layers	
11	S rim (20, 9); SW Rift Zone; 2 cm (9)	Pink, compact, continuous, even, very thin bed; planar or mantling	Ash; sparse ash-coated fine lapilli	L, C, A?	Sharp base; not always distinguishable from 12	Accretionary lapilli common
	Small-volume lava flow in Kau Desert					

Table 2 (continued)

Layer	Distribution, T_{max}[a]	Color, fabric, and structure	Grain size[b]	Components[c]	Contacts	Other
Middle, heterogeneous, ash and lapilli beds						
10	S rim; 102 cm (9, 20)	Olive-brown laminae and thin beds interbedded with dark-gray, laminae and thin beds; Top, lenticular, wavy and broad, low-angle cross-lamination; Base, continuous, even, planar bedding	Coarse ash interbedded with well-sorted fine lapilli	Ash: J Lapilli: L, C, J	Top commonly eroded (e3); separated from layer 9 by reworked interval (e.g., 9) or by erosion surface (e.g., 40), or gradational contact (e.g., 20)	Uncommon accretionary lapilli (e.g., 8); cannot distinguish from layer 8 where layer 9 is missing (e.g., 41)
9	Widespread, S and SW rim, SW Rift Zone, Mauna Loa Scenic Road, Golf Course Road; 177 cm (8)	Top, (1) olive-yellow, compact, thin beds interbedded with (2) dark-gray, loose laminae; continuous, even, planar Middle, compact, internally laminated or cross-laminated thin bed Base, (1) pale-olive, compact thin beds interbedded with (2) gray, loose laminae; continuous, even, undulating	Top, finer; Base, coarser; (1) poorly sorted ash with scattered pumice and scoria lapilli; (2) well-sorted fine lapilli	Thin beds: J ≫ L, C laminae: mixed	Contact with layer 8 is gradational and poorly defined; bedding locally deformed beneath lapilli	Abundant accretionary lapilli in thin beds, ± vesicles; ≡ lower accretionary lapilli layer at "Footprints"
8	S rim, SW Rift Zone; 110 cm (20)	Top, olive-yellow, diffuse lamination or thin bedding, common cross-lamination; Base, purplish brown, non-bedded to poorly thin bedded, laminated or cross-laminated; discontinuous	Top, poorly sorted ash and lapilli Base, very poorly sorted ash and lapilli	Top, ash J > L, C; lapilli L > J; Base, ash mixed; lapilli L;	Top, poorly defined gradational contacts; Base, lower contact is commonly erosional; confined to depressions	Uncommon accretionary lapilli (e.g., 14); vesicles, intraclasts of layer 7 (e.g., 14, 41)
7	Most rim sections; Kau Desert, SW Rift Zone, part of Mauna Loa Scenic Road; > 44 cm (8)	Purple, compact, thick bed with internal laminae, very thin and thin beds; continuous even, planar; at base, speckled, pinkish, loose, normally graded, continuous lamina	Fine ash, some laminae of coarse ash; graded coarse to fine ash at base	mixed J, L, C, A?	Gradational to sharp, conformable contact with layer 6; top contact is erosional	Abundant accretionary lapilli and vesicles; flame structures (e.g., 41) sparse fresh, black scoria fine lapilli (e.g., 41)
6	Kau Desert; Chain of Craters Road; 41 cm (6)	Predominantly black, loose, internally graded (normal or symmetric reverse-normal), continuous, even, mantling bed	Well-sorted lapilli to coarse ash; sparse blocks	Black scoria ≫ L, C	Separated from layers 1–4 by erosion surface, (e1), ± reworked interval	± Yellow, ash coated pumice; ± Red scoria lapilli at top

Table 2 (continued)

Layer	Distribution, T_{max}[a]	Color, fabric, and structure	Grain size[b]	Components[c]	Contacts	Other
Lower, well-bedded, vitric ash						
5	Section 27, NE rim; > 140 cm (27)	Olive-brown, massive, discontinuous bed	Very poorly sorted, ash, lapilli and blocks; matrix-supported	Mixed (ash mostly J; lapilli and blocks J + L)	Not established	Scattered accretionary lapilli in lower part; ash coating on black scoria lapilli
4	Kau Desert; 270 cm (9)	Yellow, compact, continuous, planar, even laminae (some 1 mm thick)	Fine and coarse ash	J	Top contact erosional, locally reworked	mm-sized, rounded, yellow pumice grains; similar to layer 2
3	Kau Desert; 250 cm (9)	Main upper part, (1) dark-gray, loose, very thin to thin beds, interbedded with (2) gray-olive, compact, laminae and minor thin beds; continuous, planar, even; includes one low-angle truncation; Lower quarter, as above with additional interbedded (3) olive, compact, medium, beds	(1) well-sorted fine lapilli; (2) coarse ash; (3) fine and coarse ash with sparse lapilli	(1) mixed (2) J ≫ L, C (3) J	Contact with layer 4 is gradational, or sharp and planar, and conformable; locally separated by thin reworked interval; lower part is separated from the rest by a low-angle truncation	Coarser than layers 2 and 4; ± vesicles in ash beds; mm-sized accretionary lapilli and ash-coated pumice lapilli in the lower part
2	S and SW rim, SW Rift Zone, Kau Desert; 250 cm (20)	Olive, compact, continuous, even to undulating laminae; single thin bed at base; internal low-angle truncations (e.g., 9)	Well-sorted fine and coarse ash; bed at base is poorly sorted ash to fine lapilli	J ≫ L, C	Separated from layer 3 by cross-laminated, reworked interval, or low-angle erosion surface	Finer and poorer in lithic components than layer 1 and 3; accretionary lapilli near top at location 20
1	SW rim, SW Rift Zone; 194 cm (41)	Upper two-thirds, (1) dark-gray, loose laminae and very thin beds, interbedded with (2) olive, compact laminae; continuous, even, diffuse; Lower third, (3) dark-gray, loose laminae, interbedded with (4) pale-olive, compact laminae and thin beds; continuous, even, mostly planar, diffuse	(1) well-sorted fine lapilli, (2) coarse ash ± pumice lapilli; (3) coarse ash; (4) fine ash	(1), (3), mixed (2), (4), J ≫ L, C	Separated from layer 2 by low-angle erosion surface; lower part separated from upper part by low-angle erosion surface ± reworked interval (e.g., 41), or else contact is gradational; in most sections, layer 1 lies on lava or basal reticulite	Not present in all sections; internal low-angle truncations locally within lower part (e.g., 48)
0	NW rim only (at locations 21 and 68); 6 cm	Pink, internally massive, thin bed	Fine ash	L, A?	Apparently mantling reticulite below; top contact may be erosional	Locally eroded, discontinuous; abundant accretionary lapilli and vesicles

[a] T_{max}, maximum thickness; (14 A), location where T_{max} was measured; [b] grain size in proximal sections, fine lapilli 2–16 mm; [c] *L*, dense lithic and red scoriaceous clasts; *C*, crystal fragments, principally olivine and/or feldspar; *A*, pale, dull, altered (?) ash; *J*, juvenile pyroclasts (glassy ash, fresh scoria, pumice); mixed, combination of L, C, A and J

laminae ($\leqslant 1$ cm) and very thin beds (1–3 cm) are ubiquitous.

Given all these features, the subdivision into four layers is based mainly on subtle grain size differences. Layers 2 and 4 are overall finer, comprising laminae of vitric coarse and fine ash, whereas 1 and 3 include very thin beds of fine lapilli richer in nonjuvenile components. No single mapped section contains all four layers. The four layers cannot be distinguished in very thin, distal, or poorly exposed sections.

The middle, heterogeneous, ash and lapilli division

The bulk of this part of Keanakakoi ash (layers 9, 10) is dominantly juvenile, olive ash and fine lapilli, with well-developed lamination or thin bedding similar to the lower division. However, like the upper division, the middle division includes thin to medium ash beds with abundant accretionary lapilli (layer 7, within layer 9), cross-bedded intervals (parts of layers 8 and 10), and lithic-rich layers (part of layer 8, layer 7). In addition, layer 6 has features which set it apart from all the other layers; specifically, layer 6 is composed of black and gray, well-sorted scoria in a single, internally massive or graded, even, continuous bed that mantles the depositional surface. At the base of layer 7, there is a very thin, but remarkably widespread deposit of reddish, speckled, well-sorted, coarse ash. The rest of layer 7 is a very compact, purple, continuous, medium-thickness bed of fine ash rich in accretionary lapilli and internally bedded. This distinctive pair of layers (6 and 7) provides a most useful marker around much of the caldera rim and in the southern and southeastern areas, and it constitutes a striking departure from both the lower division and the remainder of the middle division.

The lower part of layer 8 is purplish and lithic rich like layer 7, but is coarser, poorly bedded or cross-laminated, and laterally discontinuous. The upper part of layer 8 is olive-brown, richer in juvenile components, and in places contains accretionary lapilli. At the top it grades into layer 9 with an increase of juvenile components, decrease in grain size, and development of pla-

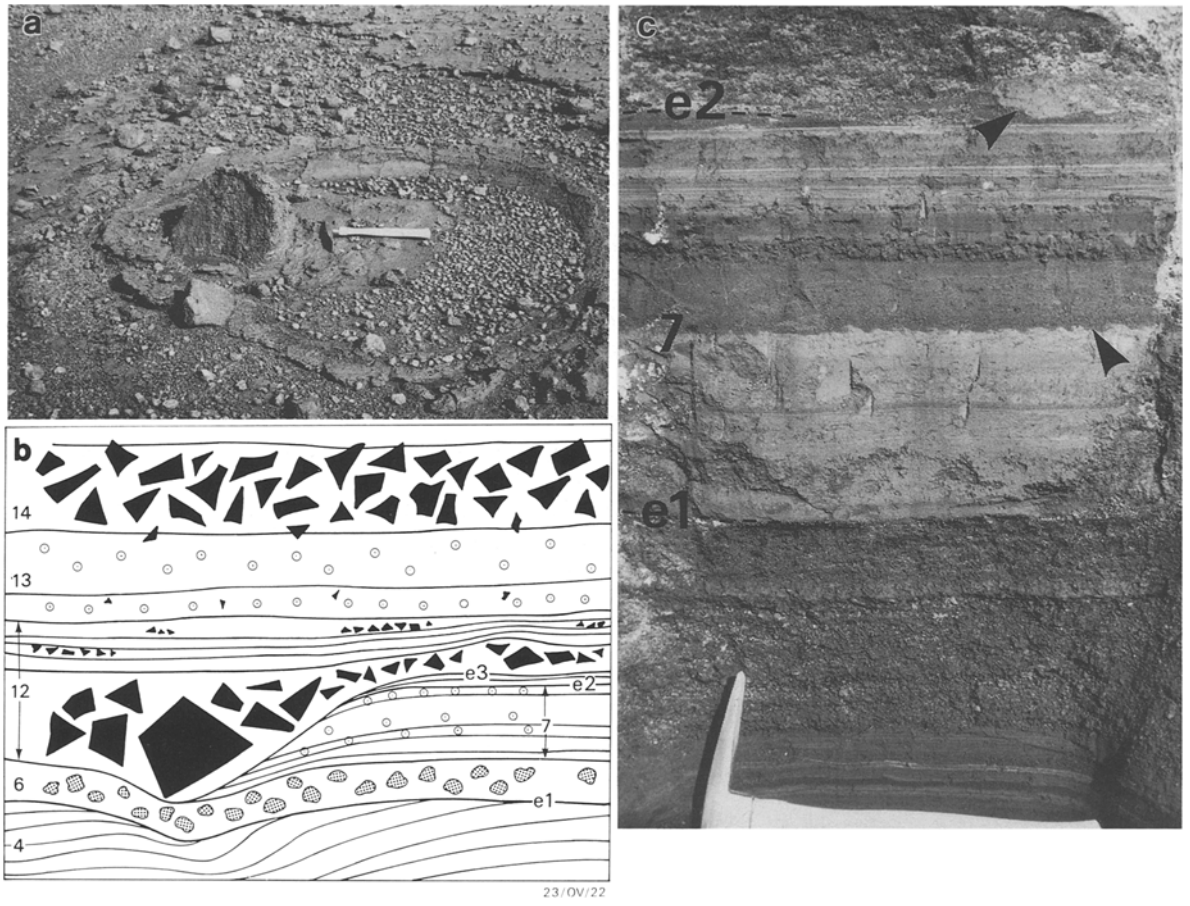

Fig. 3. **a** Layer 16 block within original impact crater at locality 46, approximately 1 km southwest of Kilauea caldera rim. The hammer is 33 cm long; its handle is parallel to 060° and points toward the caldera. **b** Section through Keanakakoi ash at locality 55, Kau Desert, about 500 m south of Kilauea caldera rim. Layer 6 scoria fall of the middle division overlies an erosion surface, e1, that cuts down into layer 4 of the lower division. Note also the two higher erosion surfaces, e2 and e3. The section shows the topmost one metre of the exposure. **c** Intraclast (*upper arrow*) of layer 7 accretionary lapilli ash within reworked deposits at the base of layer 8 in a section through Keanakakoi ash at locality 41 approximately 600 m southwest of Kilauea caldera rim. Erosion surface e2 separates layers 7 and 8, and e1 separates layers 7 and 3. Note flame structures (*lower arrow*) between thin beds within layer 7

nar, even, continuous bedding. The main feature of layer 9 is the presence of thin to medium beds packed with accretionary lapilli. One of these extends at least to the "Footprints" locality in the Southwest Rift Zone; its upper surface is remarkable in preserving fossil human footprints and dessication cracks first reported by Jaggar (1921). Layer 10 also includes a small number of well-sorted, thin, continuous, fine lapilli beds, and unlike layer 9, the topmost part has low-angle cross-bedding and wavy bedding in many exposures.

The upper, lithic-rich, block and ash division

The six uppermost layers of Keanakakoi ash (11–16) are conspicuously lithic rich and display a wide range in grain size, sorting, and bed forms. Two layers (12 and 13) each include three subdivisions easily identified in proximal areas, giving a total of ten depositional units. In simplest terms the sequence is composed of four block and lapilli beds (12b, 13b, 14, 16) intercalated with three separate beds of ash (11, 13a, 13c) and three cross-bedded ash and lapilli intervals (12a, 12c, 15).

The ash beds are pinkish orange, compact, even, and continuous, and mantle irregularities on the underlying surface. Layer 13 ash beds have delicate internal laminae and include abundant accretionary lapilli and sparse lithic lapilli. At the "Footprints" locality in the Southwest Rift Zone, human footprints are impressed into the top surface of layer 13. The block and lapilli beds of the upper division are clast supported, matrix poor, and laterally continuous. Bed thickness variation ranges from uneven in rim sections where blocks occur and where bedding sags are infilled, to even in more distal areas where the sorting of clasts is better and blocks are absent. Of the four block beds, layer 14 is the thickest and most widespread. The topmost block "bed", layer 16, is more accurately described as a scattering of lapilli and blocks at the same stratigraphic level and is responsible for the numerous impact sags on the surface close to the caldera rim in the Southwest Rift Zone (Fig. 3a). Distinguishing between the upper two block layers (14 and 16) is possible only where layer 15 occurs.

The upper and lower parts of layer 12 and layer 15 comprise wavy, lenticular, and cross-bedded ash and fine lapilli. In all three cross-bedded intervals, but particularly in layer 15, even, continuous laminae and very thin beds of accretionary lapilli-bearing fine ash separate some of the bed sets (cf. Walker 1984). In some sections, lapilli in layer 12c (e.g., section 40) and layer 15 (e.g., section 12) are coated with fine ash. Foresets of well-defined cross-bed sets have unidirectional dip azimuths, indicating downcurrent movement radially away from the caldera rim. The basal contacts of the layer-12 cross-bedded intervals are commonly erosion surfaces ranging from shallow disconformities to spectacular, deeply incised channels along the southern rim (sections 9, 55, 56; Fig. 4a). Layer 15 typically has a gradational lower contact with layer 14; the top contact is a regularly undulating dune surface (e.g., sections 12, 18, 24, 21) where not modified by erosion or sagged beneath blocks belonging to layer 16.

Throughout the upper division, clasts coarser than about 1 mm are accessory lithics, principally dark-grayish or reddish basaltic lava accompanied by variable amounts of olivine and feldspar crystal fragments. Juvenile magmatic clasts have not been identified among the components of this size and are apparently limited to finer ash fractions. Ash in the cross-bedded and accretionary lapilli-bearing layers (11, 12a, 12c,

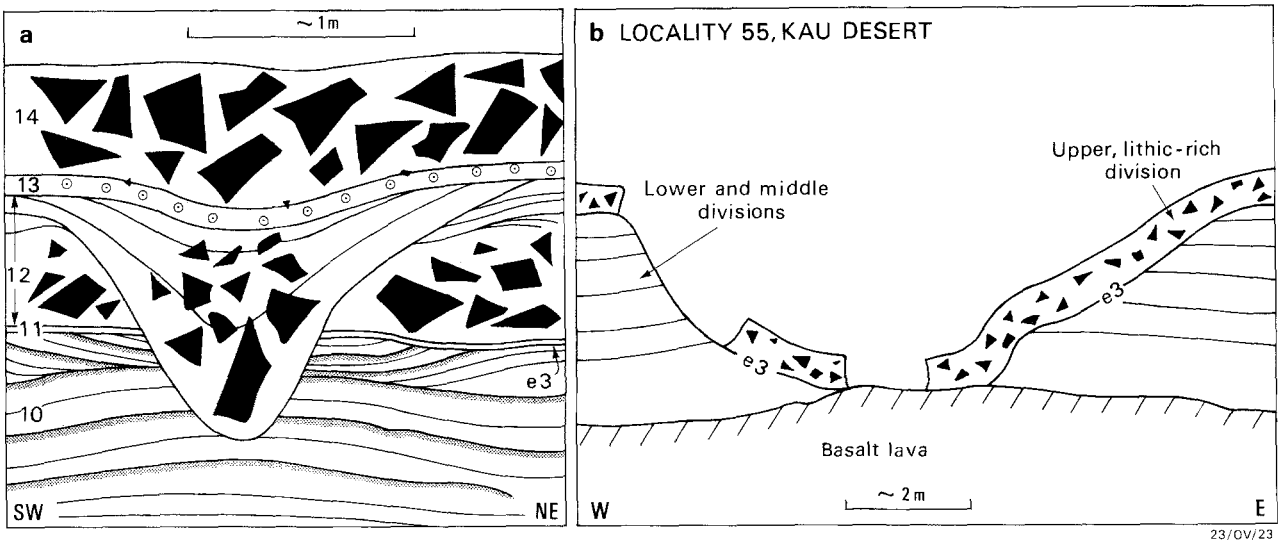

Fig. 4. a Section through Keanakakoi ash at locality 9 on the southern rim of Kilauea caldera. A U-shaped erosion surface within the upper lithic-rich division (base of 12c) cuts deeply into underlying ash of the middle division where it merges with erosion surface e3. The view is upcurrent, toward the caldera. **b** Profile of a modern gully cutting Keanakakoi ash in the Kau Desert near locality 55 showing the similarity of its shape and the e3 erosion surface. The upper lithic-rich division drapes the undulating e3 surface. The view is toward Kilauea caldera about 500 m south of the rim

13a, 13c, 15) is distinctly purplish or pinkish. The color is imparted by reddish particles derived from oxidized scoria or lava, combined with very fine, pale-grayish, dull ash; other components are crystal fragments (olivine, clear feldspar) and dull, gray-black, basaltic lithic grains. The very fine, pale ash appears to be derived from altered rocks (cf. Heiken and Wohletz 1985, p. 15). Juvenile ash pyroclasts were confidently recognised only in the cross-bedded intervals, ranging from conspicuous to trace proportions. However, it cannot be assumed that these pyroclasts were a primary component of the ejecta, as is explained below.

In most sections there is a subtle color change coinciding closely with the base of layer 11 from olive-brown below to pinkish-purple above, reflecting the changeover from dominantly juvenile to dominantly lithic ash fractions. However, along part of the Southwest Rift Zone (sections 14A, 40, 41, 42, 43, 48; Fig. 1), only the upper part of layer 12a is pinkish-purple, the lower part being olive-brown. Close to the caldera rim (e.g., section 14A) layer 11 is missing, and the base of layer 12 is erosive into the underlying olive, ash-rich beds. It thus appears that the juvenile component at the base of 12a in Southwest Rift Zone sections was scavenged from lower parts of Keanakakoi ash at the rim and more proximal locations, diluting the initially lithic-rich ejecta, and then the mixture was deposited farther downcurrent. That is, the juvenile ash at the base of layer 12a is not considered to be a primary component, but rather is accidental (Wright et al. 1980) and intraformational in origin. The upper part of layer 12 (12c) also contains trace amounts of juvenile pyroclasts, but the coincidence with cross bedding again means that it cannot be assumed that these are primary components and instead are most likely to have been recycled from older Keanakakoi ash deposits.

Other layers

Two layers of very restricted extent have not been included in the three subdivisions described above. Layer 0, limited to sections 21 and 68 close to the northern rim of Kilauea, is a single thin bed of pink, fine ash with accretionary lapilli and vesicles. Layer 5, identified only in section 27, is a massive, poorly sorted, thick bed composed of both juvenile (yellow ash, pumice, ash-coated black scoria) and lithic (blocks and lapilli) fragments.

A thin lava flow is locally intercalated with the Keanakakoi ash in the Kau Desert (Stone 1926; Stearns and Clark 1930; Christiansen 1979; Decker and Christiansen 1984), and apparently erupted from a fissure located about 1.25 km from the caldera rim. It evidently occurs at or near the top of the middle division between layers 10 and 11 (Fig. 2).

Shapes of juvenile ash pyroclasts

Juvenile ash is the principal component of the lower and middle divisions of Keanakakoi ash; the exceptions are layer 6 which is generally coarser, layer 7 which is rich in altered lithic ash, and the lower part of layer 8 which is both coarser and lithic rich. Ash samples were examined with a binocular microscope in order to determine the shapes of the juvenile pyroclasts. Five main shapes occur:

(1) blocky or platy, nonvesicular fragments of glossy black (tachylite?) or clear yellow (sideromelane) glass;

(2) blocky fragments of glossy black glass with isolated, small, spherical vesicles bounded by planar or smoothly curving surfaces;

(3) irregularly shaped, highly vesicular, glossy, yellowish glass fragments with very high surface area; many vesicles are in contact and deformed;

(4) cusps and spines of nonvesicular, glossy yellow glass;

(5) fragments of Pele's hair and Pele's tears.

Shapes (1) and (2) are similar to the type-I pyroclasts of Wohletz (1983). Shape (3) may include both true pumice and type-III mosslike pyroclasts of Wohletz (1983). Shape (4) matches the type-V shards described by Wohletz (1983). Pele's hair and Pele's tears are the typical products of in-flight solidification of lava spray ejected during Hawaiian or Strombolian-style eruptions (Walker and Croasdale 1972). Pyroclasts with shapes (4) and (5) are much less abundant than the other three, and shapes (1) to (4) occur together in the same samples.

Blocky, poorly or nonvesicular pyroclasts and high-surface-area, mosslike pyroclasts are considered to be diagnostic of magma-water interaction during fragmentation and prior to explosive ejection (Wohletz 1983). Broken bubble-wall shards and the juvenile pumice lapilli scattered through the lower and middle divisions of Keanakakoi ash indicate that for parts of the magma this interaction was delayed until after vesiculation. Such a sequence is consistent with the suggestion by Wohletz (1983, 1986) that mixing of magma and water to produce hydrovolcanic explosions is enhanced if the magma is partly fragmented to begin with.

Lateral correlations and distribution of Keanakakoi ash

Figure 5 correlates the measured sections. The southern and southwestern rim exposures are the most complete and thickest (>4 m to 11 m). The deposits are much thinner (<2 m) in the remaining rim sections, as a result of both absence of some layers and reduced thickness of those present. Stratigraphic subdivision and correlation are most difficult around the northern to eastern arc where the ash is covered with dense vegetation and suitable exposures are uncommon.

The upper division occurs all around the rim, and two layers (12, 14) are present in every rim section. Both the middle and lower divisions are missing at different sites along the perimeter. The upper division is also continuously represented (mainly by layers 13 and/or 14) along four of the six radial traverses (Southwest Rift Zone, Kau Desert, Chain of Craters Road and

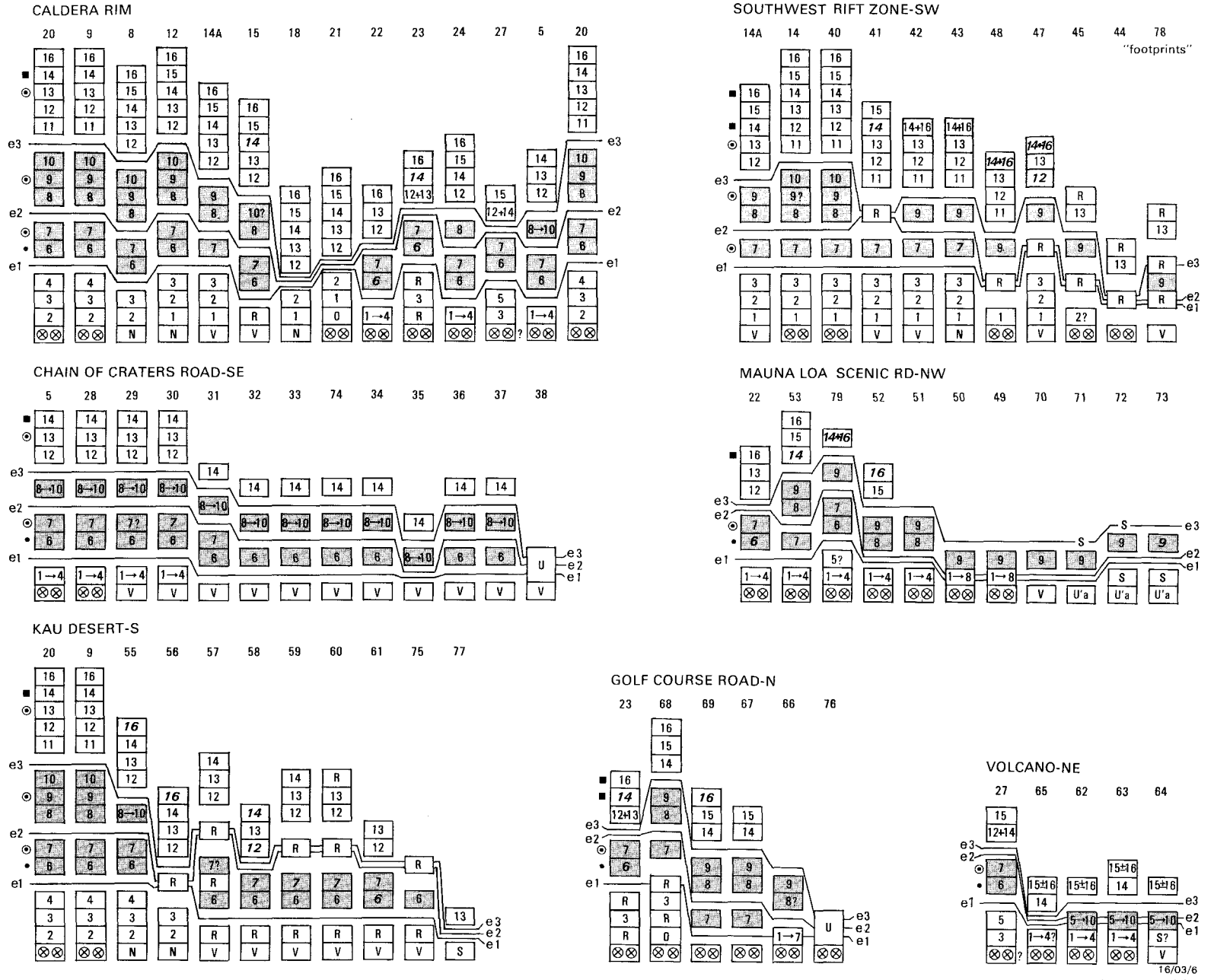

Fig. 5. Correlation of layers within Keanakakoi ash along radial and rim traverses. Section locations are shown on Fig. 1. *N,* base not exposed; *V,* basaltic lava flow; *R,* reworked ash; *S,* soil; *U'a,* Uwekahuna Ash Member; *U,* undifferentiated ash deposit. *e1, e2,* and *e3* are erosion surfaces. Numerals in italics indicate layers present only in trace amounts. Layers of the middle division are *shaded.* ⊗⊗, basal reticulite; ●, scoria fall; ⊙, accretionary lapilli ash fall; ■, block fall

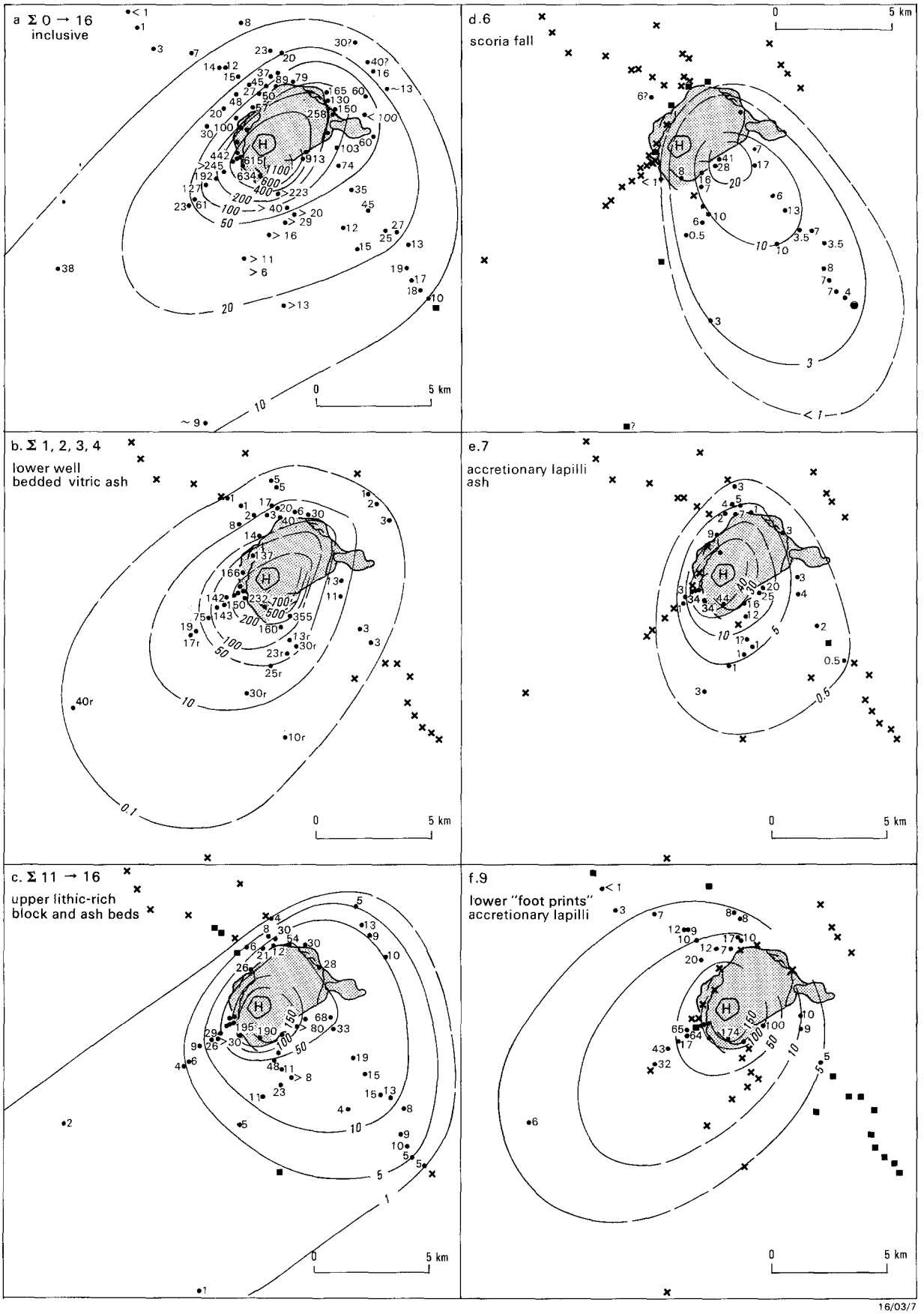
a Σ 0 → 16
inclusive
d.6
scoria fall
b. Σ 1, 2, 3, 4
lower well
bedded vitric ash
e.7
accretionary lapilli
ash
c. Σ 11 → 16
upper lithic-rich
block and ash beds
f.9
lower "foot prints"
accretionary lapilli
0
5 km
16/03/7

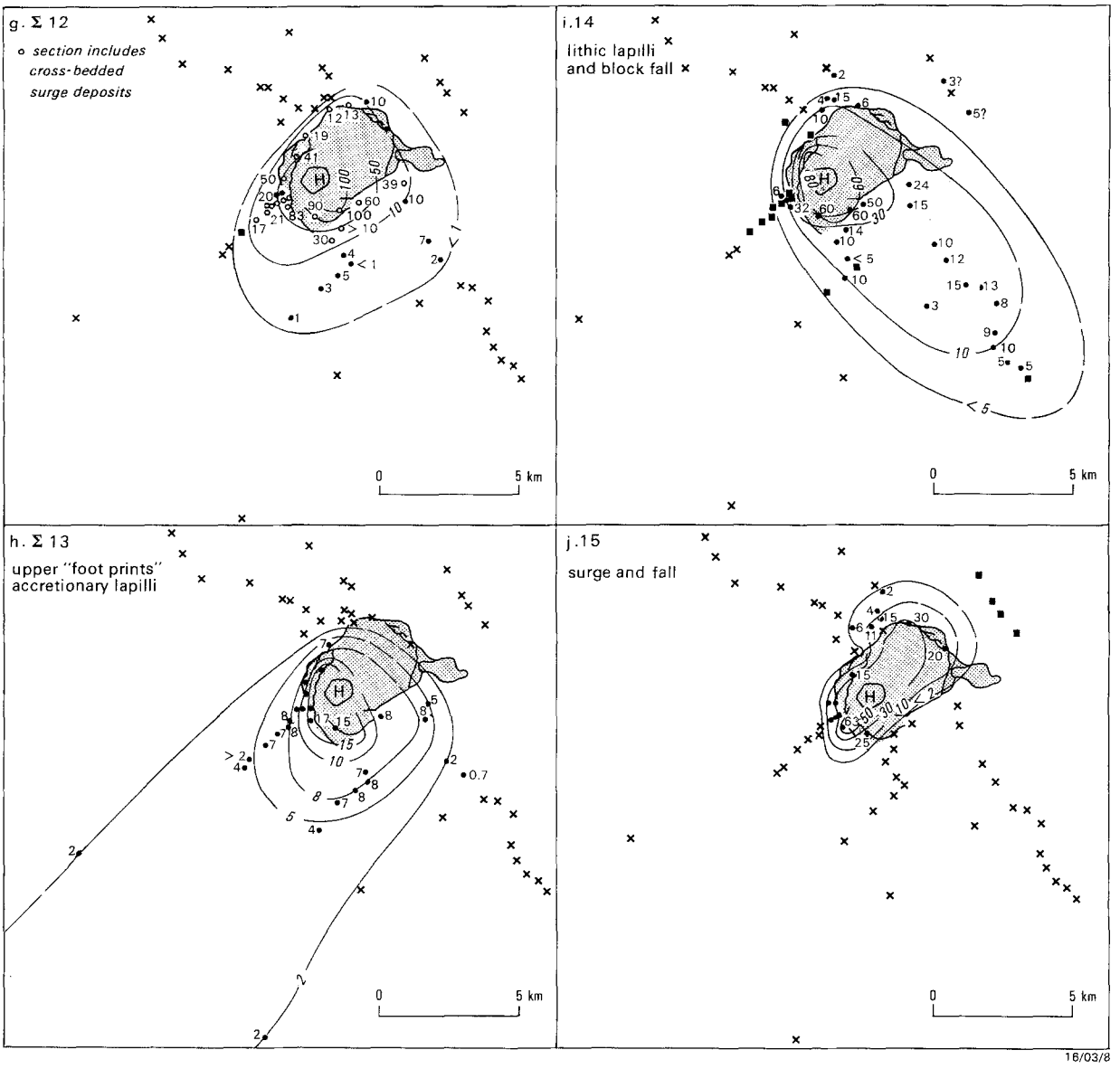

Fig. 6. Isopachs in centimetres for Keanakakoi ash and selected component layers. ×, layer not present; ■, layer not identified as a separate unit or thickness not recorded; *r*, thickness measurement includes reworked ash; *H*, Halemaumau

Volcano; Fig. 5). Layers of the middle division are even more widespread, occurring in every section along all but one (Volcano) of the radial traverses. Layers 6 and/or 7 are consistently exposed in the Kau Desert and Chain of Craters Road traverses, whereas layer 9 is the principal representative in the Southwest Rift Zone, Mauna Loa Scenic Road, and Golf Course Road traverses. The lower division is not continuous as a primary deposit in any of the radial traverses, and thins rapidly to zero outward from the caldera rim (e.g., Chain of Craters Road traverse), or else is reworked (e.g., Kau Desert and Southwest Rift Zone traverses).

The isopach map (Fig. 6a) for the total Keanakakoi ash indicates an overall bias in dispersal toward the southwest, but masks the divergent dispersal directions shown by some layers. In particular, layers 6, 7, 12, and 14 are distributed more toward the southeast or south, and layer 15 has a northern as well as a southwestern lobe. The isopach maps, isopleth maps of selected layers (Fig. 7), and inferred dispersal axes based on these (Fig. 8) confirm the conclusion of Stearns and Clark (1930) that all the component layers of Keanakakoi ash originated from a vent (or vents) in the vicinity of the modern Kilauea caldera.

When traced laterally away from the caldera rim, each layer maintains a consistent set of textural and compositional features, though systematically becomes finer grained. This is most marked for the block-rich beds of the upper division, but still detectable in the ash-dominated layers. Accretionary lapilli in fine ash beds also decrease in size outward from the caldera (Fig. 7e, f).

Erosion surfaces within Keanakakoi ash

Almost every layer of the lower and middle divisions is

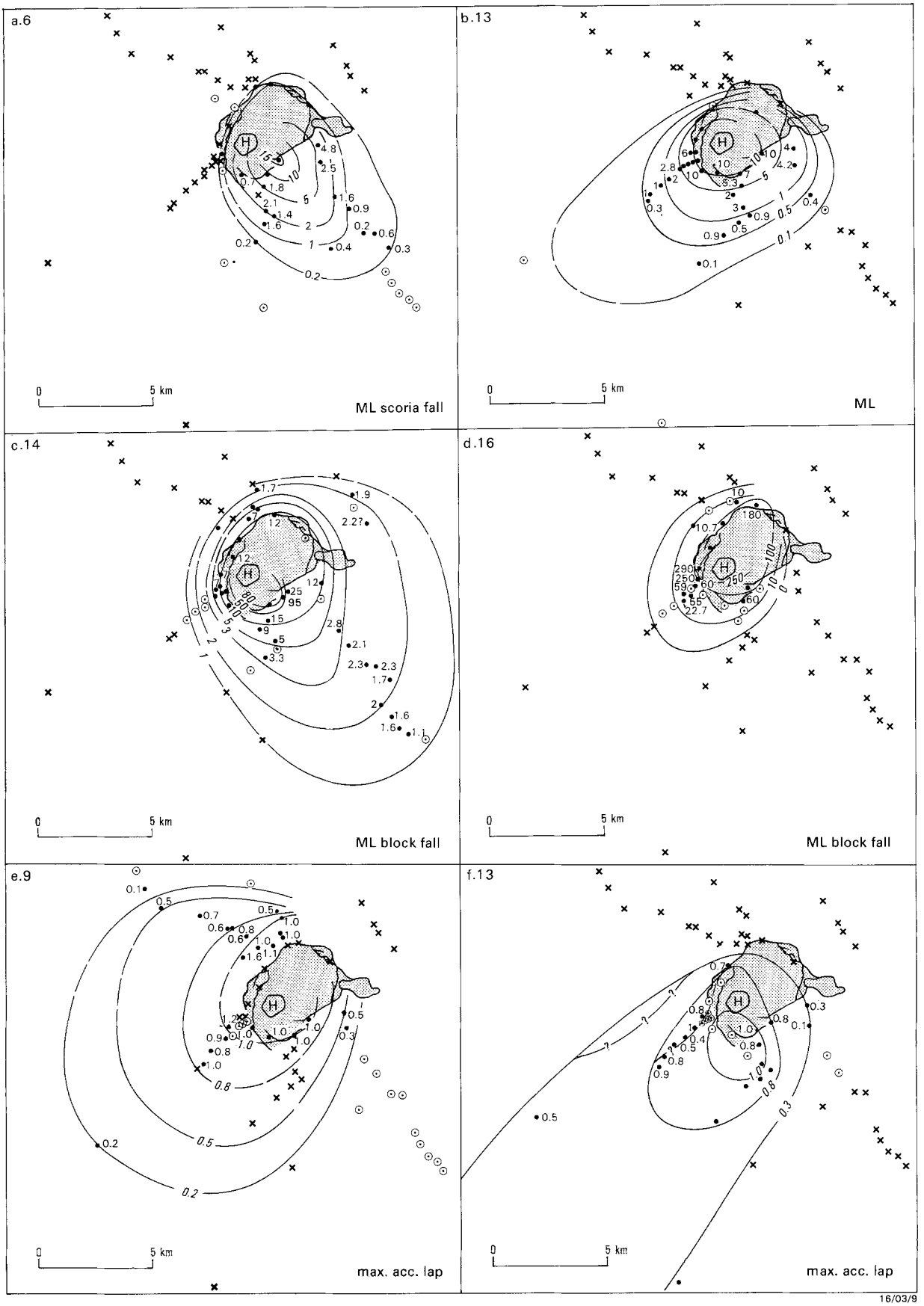

Fig. 7. Isopleths in centimetres for maximum dimensions of dense lithic clasts or accretionary lapilli in selected layers of Keanakakoi ash. ×, layer not present; ⊙, lithics or accretionary lapilli not present in the unit, or size not recorded

bounded by an erosion surface ranging in importance from barely incised local discordances within otherwise conformable sequences, to deeply incised, widespread unconformities, in places associated with reworked deposits. The main unconformities occur between layers 4 and 6 (e1, separating the lower and middle divisions), between layers 10 and 11 (e3, separating the middle and upper divisions), and e2 (within the middle division; Fig. 2).

The timing and significance of the lowermost erosion surface (e1, Figs. 2 and 5) are evident from the Kau Desert traverse. At the caldera rim (section 20) layers 6 and 4 are conformable, or else separated by a thin (10 cm), slightly reworked interval (section 9). About 500 m farther south (section 55) layer 6 overlies a disconformity excavated into layer 4 (Fig. 3b). In the next section (56) another 500 m to the south the thickness of the lower, well-bedded ash is greatly reduced, and layer 4 almost eliminated. At the base of all remaining Kau Desert sections (except the most distal, 77), very well sorted, cross-bedded, juvenile ash underlies layer 6. The composition of this ash is very similar to that of layers 1–4 in that juvenile particles (olive glass) predominate and are accompanied by lithic and crystal fragments. The cross-bedded intervals are discontinuous: they infill depressions and pinch out at highs in the substrate. Cross-beds are steep (at or near angle of repose), and foreset dip directions are variable in single exposures. This cross-bedded ash is evidently the redeposited equivalent of layers 1–4, and the principal agent responsible for redeposition is inferred to have been wind. The break between emplacement of the lower division and layer 6 thus had to be sufficiently long to allow aeolian erosion, transportation, and redeposition of much of the proximal layer 1–4 section.

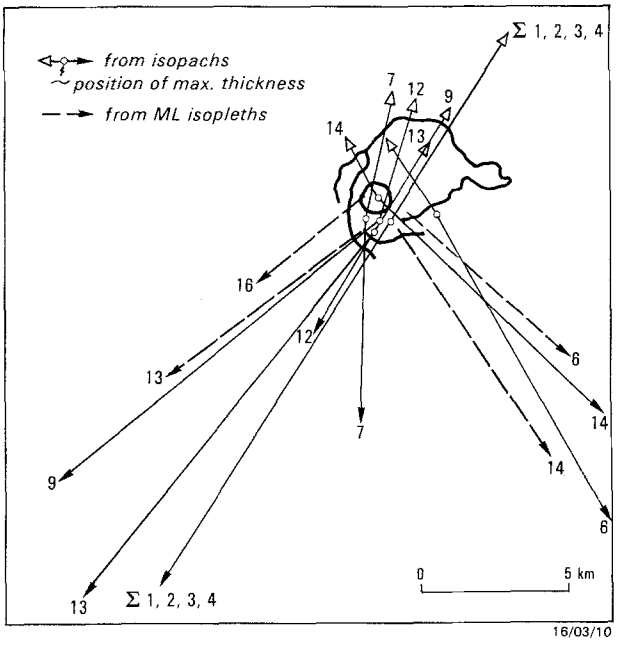

Fig. 8. Dispersal axes of Keanakakoi ash and of selected component layers based on the shapes of isopach and isopleth maps

The tradewinds are dominantly northeasterly and yet both the principal area of aeolian reworking of layers 1–4 and the dispersal of layer 6 are more southern and southeastern, respectively, from Kilauea (Fig. 6b, d). Evidently the layer 4–layer 6 break was long enough to accomodate shifts from the trades to these directions. The erosion and reworking were probably not confined exclusively to the south-southeastern corridor: in sections along the Southwest Rift Zone (14A–43, Fig. 1), layer 7 overlies an erosion surface excavated into the lower, well-bedded ash. This surface cannot be uniquely constrained as the same pre-6 surface in the Kau Desert, as it could be the result of a post-6, pre-7 event. However, there is very little evidence elsewhere of a break between these two layers, and the absence of layer 6 is due to the off-dispersal axis position, rather than to pre-7 erosion. It is thus apparent that a single pre-layer-6 erosion and reworking episode has affected the southwest and southeast sectors, the southwest being consistent with the typical tradewind pattern and the southeast indicating intermittent deviations from the norm.

Erosion surface e2 separates layers 7 and 8 (Fig. 2). On the southern and southwestern rim of the caldera (e.g., sections 20, 9, 8, 14, 40, 41; Fig. 5) layer 7 has been locally eroded and then overlain by reworked deposits at the base of layer 8; intraclasts of layer 7 are scattered within layer 8 close to the contact (e.g., sections 14, 41; Fig. 3c). The reworked deposits comprise discontinuous, cross-bedded, lithic lapilli and mixed juvenile-lithic coarse ash, mostly confined to depressions in the underlying erosion surface. Both the erosion and reworking were probably the result of surface water wash during and following rain storms after layer 7 was emplaced. Rain storms are common at Kilauea's summit and in this case, it is also likely that steam condensed from the eruption column contributed. Beyond the limit of dispersal of layer 7 along the Southwest Rift Zone traverse (Fig. 5), e2 cannot be distinguished from e1, and their relative roles in eroding and reworking of the pre-layer-6 section is unknown.

The upper division overlies a widespread erosion surface, e3, established in exposures at the southern rim and extending into the Kau Desert and the distal Southwest Rift Zone. At the southern rim (sections 20, 9; Fig. 5) sections are nearly complete up to and including layer 10. At a distance of about 500–700 m south of the rim in the Kau Desert, the pre-layer-12 deposits rapidly thin (section 55), and in places layer 12 rests on layer 4 or deeper layers (section 56). The lithic-rich layers drape a deeply incised and irregular to undulating erosion surface, similar in shape to modern rainwater runoff gullies (Fig. 4b). Where layers 7 to 10 are missing, especially in more distal Kau Desert sections, e3 merges with e2.

At the southern rim (near sections 9, 20) there are examples of smooth, U-shaped erosion surfaces that begin within layer 12 (at the base of 12a or in 12c) and can be traced down into layer 10 or deeper where they are indistinguishable from e3 (Fig. 4a). Decker and Christiansen (1984) have related erosion of these chan-

Table 3. Summary of interpreted emplacement processes and eruption styles for the Keanakakoi Ash Member

	Layer	Emplacement process	Eruption style	Evidence for H_2O involvement
000	Golden pumice	Pumice fall	Explosive magmatic	None
16	Lapilli & blocks	Lapilli & block fall	phreatic	Abundant accretionary lapilli ± vesicles ± ash-coated lapilli in fine ash beds; surge deposits; paucity or lack of juvenile magmatic components; hydrothermally? altered ash
15	Cross-bedded ash & lapilli	Surge (+ cosurge ash fall)	Fatal eruption-column collapse?	
14	Lapilli & blocks	Lapilli & block fall		
13 c	Fine ash ± accretionary lap.	Rain flushed ash fall	"Wet"	
13 b	Lapilli & blocks	Lapilli & block fall		
13 a	Fine ash + accretionary lap.	Rain flushed ash fall	"Wet"	
12 c	Cross-bedded ash & lapilli	Surge (+ cosurge ash fall)	Eruption-column collapse?	
12 b	Lapilli & blocks	Lapilli & block fall		
12 a	Cross-bedded ash & lapilli	Surge (+ cosurge ash fall)		
11	Fine ash + accretionary lap.	Rain flushed ash fall	"Wet"	
e3	Lava	Flow	Effusive magmatic	None – separate fissure vent
10	Well-bedded ash & fine lapilli ± acc. lap; J>L	Ash fall, rain flushed ash fall ± wind-drifted fall or surge?	Phreatomagmatic	Fine grain size, even near source; abundant accretionary lapilli ± vesicles; palagonite alteration of glassy pyroclasts; blocky shapes of juvenile pyroclasts
9				
8	Cross-bedded ash & lapilli	Reworked-surface wash, fluvial	n.a.	
e2				
7	Fine ash + acc. lap; J+L	Rain flushed ash fall	"Wet" phreatomagmatic	
6	Well-sorted scoria lapilli	"Dry" scoria fall	Explosive magmatic (Strombolian-style)	None – separate "dry" vent?
e1				
5	Poorly sorted ash → blocks	Redeposited slump?	n.a.	Fine grain size, even near source; accretionary lapilli, ash-coated lapilli ± vesicles; palagonite alteration of glassy pyroclasts; blocky shapes of some juvenile pyroclasts; lamination
4	Well-bedded ash; J>L	Ash fall (+ minor rain flushing; + minor wind drifted ash fall)	Relatively "dry" phreatomagmatic	
3				
2				
1				
0	Fine ash + acc. lap (L?)	Rain flushed ash fall	"Wet" phreatic	Acc. lap., vesicles, fine grain size
000	Basal reticulite	Pumice fall	Explosive magmatic	None

nels to events associated with the emplacement of the upper, lithic-rich beds (in particular, layer 12). Hence they cannot be taken to indicate significant post-e3 breaks in the accumulation of the deposits. Also, elsewhere around the caldera the upper division of Keanakakoi ash lacks evidence for interruptions.

The duration of the break represented by e3 is inferred from distal sections of the Southwest Rift Zone; relationships at section 78 ("Footprints" locality, Figs. 1 and 5) are particularly clear. Most exposures there include two very thin beds of accretionary lapilli-bearing fine ash, each underlain by cross-bedded, well-sorted, mixed juvenile-lithic coarse ash interpreted to be aeolian deposits from the erosion and reworking of the tephra from more proximal localities. Correlations through the Southwest Rift Zone traverse show that the accretionary lapilli beds are the distal representatives of layer 13 (upper) and layer 9 (lower). The aeolian deposits below layer 9 are therefore the reworked equivalents of layers 1 to 7 inclusive, and are principally related to the e1 break with a possible contribution during the e2 break. The aeolian deposits between layer 9 and layer 13 are the reworked equivalents of at least layers 8 to 10 and most probably the entire pre-layer-11 section, initially emplaced at the rim but eroded and transported downwind to distal sites during the e3 break.

Emplacement processes and eruptive styles

Table 3 summarizes the interpretation of the foregoing description of the Keanakakoi Ash Member in relation to emplacement processes and eruptive styles. The bulk of the tephra was emplaced by pyroclastic fall. Rain flushing of the source ash cloud was a common occurrence. The phase represented by the upper division was

marked by the periodic ejection of much coarser debris, forming block and lapilli fall layers (12b, 13b, 14, 16), and also includes the only significant deposits emplaced by pyroclastic surges (12a, 12c, 15). Parts of the lower division (e.g., base of layer 1) and the middle division (e.g., upper layer 8, upper layer 10) may also have been generated by primary surges but their close similarity in grain size, components, and sorting to associated definite fallout ash layers suggests instead that they were deposited in windy weather conditions (cf. Carey and Sparks 1986) or were reworked by wind. Sedimentation, principally by aeolian or fluvial processes, accounts for a very small part of the accumulation except in the distal Kau Desert exposures, even though recognition of its role is otherwise important in assessing the duration of interruptions.

Most of the Keanakakoi Ash Member was produced by explosive activity. A small fissure-fed lava in the Kau Desert (Christiansen 1979; Decker and Christiansen 1984) is the only evidence of contemporary effusive eruptive behavior. Explosive activity driven by magmatic volatiles produced the basal reticulite, the golden pumice, and, during emplacement of Keanakakoi ash, a single scoria fall layer (layer 6). The eruptions responsible for all other layers were affected to lesser or greater extents by the involvement of water (Table 3). The lower and middle divisions are largely the products of strictly phreatomagmatic eruptions with abundant juvenile magmatic pyroclasts in all grain size classes. In contrast, the block fall and accretionary lapilli-bearing ash fall beds of the upper division lack juvenile magmatic components. If the conclusion reached above regarding the accidental origin of the juvenile ash found in the cross-bedded surge deposits is correct, then the entire upper, lithic-rich division can be considered as the product of phreatic eruptions.

Thus, the Keanakakoi ash eruption comprised three phases generated by two different styles of explosive hydrovolcanic activity. Initially (phases 1 and 2, lower and middle divisions), water had access to actively vesiculating and already partly fragmented magma, causing steam explosions in the conduit. Conditions were appropriate for contact-surface steam explosivity (cf. Kokelaar 1986), leading to further magma fragmentation and a combination of magmatic volatile- and steam-driven explosive ejection of pyroclasts. The uniform and relatively minor lithic content suggests that once established, open-vent conditions were maintained from a vent with stable walls. It seems that for most of first two phases the magma-water mass ratio promoted a high explosive efficiency, manifest by the thoroughly fragmented ejecta, and fluctuated only slightly, between a minimum that resulted in the fine ash and fine lapilli falls and a maximum when the "drier" scoria lapilli fall (layer 6) was emplaced. Some highly vesiculated pumice lapilli were deposited at the same time as hydrovolcanic ash. Perhaps the margins of the magma column closest to the aquifer were most affected by interaction with water whereas the central parts were freely vesiculating, at least intermittently, so that the two pyroclast types were generated simultaneously. Another possibility is that magmatic and hydrovolcanic explosions occurred in such rapid succession that pyroclasts from each were mixed in the eruption column and deposited together.

The phreatic eruptions (phase 3) that produced the upper division were presumably not aided by magmatic volatiles either as a means of initiating magma fragmentation through vesiculation or as a contributory driving force for explosions. In this case, the energy available from the explosive expansion of steam was expended mainly in the fragmentation and expulsion of wall rock, not of the magma that had simply served as a heat source in steam generation. This phase of the eruption included several major discrete explosions which may have been initiated when withdrawal of magma exposed red-hot conduit walls to water draining from the aquifer. Subsequent explosions were possibly both triggered and accompanied by vent wall collapse that disrupted the hydrothermal system surrounding the conduit. Spells between explosions probably reflect restoration of the aquifer and heating of water entrapped in the wall rocks and in the lithic debris that had accumulated in the conduit.

Some consequences of the first and second eruptive phases may have influenced the style of the activity that followed. In particular, the two phreatomagmatic phases effected the degassing and partial cooling of the magma so that what remained would have been relatively dense and likely to subside deeper into the conduit (cf. Walker 1986). Thereby the magma would have been removed from direct contact with water and rendered less efficient in transferring heat during any contact that did occur. The vent walls would have been fractured and weakened by the foregoing explosions and further destabilized if in fact magma withdrawal did take place; there would have been abundant lithic debris available during subsequent explosions. However, of overriding importance in causing the change from phreatomagmatic to phreatic activity was the decline in magma supply: the phreatomagmatic explosions involved new magma, whereas the phreatic explosions did not, although they developed from the heat released by the otherwise passive residual magma. Even though there is evidence for a pause between the phreatomagmatic and phreatic phases (e3, Fig. 2), they may both be closely related effects of a continuous process of magma withdrawal from Kilauea's summit caldera.

Kilauea in 1790

The dimensions and geometry of Kilauea's summit caldera at the start of the Keanakakoi ash eruption are unknown. The account of Dibble (1843 p. 51, 52) uses the terms "crater" and "pit" for the source of the explosions, so a well-defined depression must have existed. The margins of the modern caldera include younger fault scarps which truncate Keanakakoi ash (e.g., southeastern and northwestern sectors), and older fault scarps draped by it (e.g., northeastern and western sectors). Also, the lowest part of the modern caldera rim in

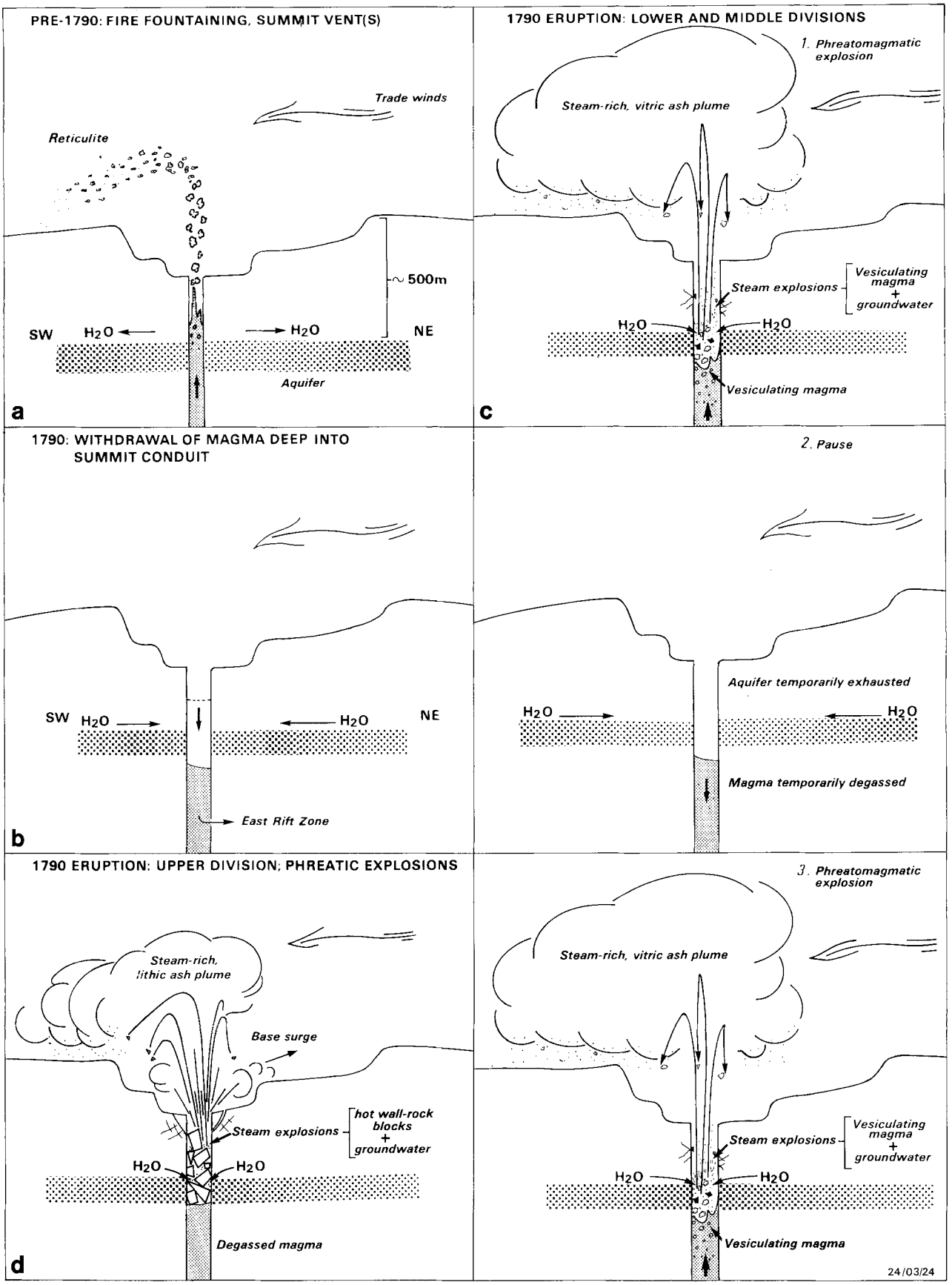

Fig. 9 a–d. Cross-section across Kilauea caldera prior to and during the 1790 Keanakakoi ash eruption. The caldera has been drawn in accord with the earliest descriptions (Ellis 1827), when the floor was deep and stepped. **a** Magmatic-volatile-driven explosive fire fountaining form a summit vent generated the basal reticulite prior to 1790. **b** Magma was withdrawn from the summit and moved to the East Rift Zone where lava eruptions occurred around 1790. Groundwater was free to infiltrate close to the summit conduit. **c** Phases *1* and *2* of the Keanakakoi ash eruption involved phreatomagmatic explosions in the summit conduit when groundwater mixed with actively vesiculating magma (*1* and *3*). Many explosions must have occurred, punctuated by pauses (*2*) reflecting the temporary depletion of groundwater and reduction of magma volatile pressure. Steam-rich eruption plumes were blown southwestward by the trade winds and frequently rain flushed. **d** Phreatic explosions during the third phase resulted from the interaction of groundwater with wall rock and lithic debris that had been heated by the largely degassed magma

the southern and southwestern sectors may also have been the lowest in 1790 because the lithic-rich surge deposits were preferentially distributed in this direction. Thus, the modern caldera is somewhat wider than the 1790 caldera as a result of subsequent formation of fault scarps outside the rim.

The basal reticulite of the Keanakakoi Ash Member indicates that "normal" summit eruptions (i.e., fire fountaining with or without generation of lava flows; Fig. 9a) took place prior to the 1790 outburst, and that magma was present at shallow levels in Kilauea's subvolcanic plumbing system (Decker and Christiansen 1984).

Lava was erupted from Kilauea's East Rift Zone around 1790 (Ellis 1827; Hitchcock 1909; Finch 1947), presumably coinciding with retreat of magma from the summit (Christiansen 1979; Decker and Christiansen 1984). The vent(s) was in the Malama district (Ellis 1827, p. 201), which ranges in elevation between about 300 m and 400 m above sea level. Lava issuing from the East Rift Zone could have drained magma from the summit storage until it reached the same level (Fig. 9b). Thus the magma column at the summit could have been as deep as 700 m below the southern rim (present elevation about 1100 m) at the time of the explosive activity of 1790. The modern groundwater table about 1 km south of Halemaumau lies 488 m below the surface elevation (Zablocki et al. 1974). The floor of Kilauea is presently relatively shallow, only about 170 m below the rim, and the caldera is quiet. However, conditions were dramatically different during the early decades of the nineteenth century when the deepest part was some 300–500 m below the rim (Ellis 1827; Douglas 1834; Dibble 1843; Brigham 1909; Hitchcock 1909), and there were several eruption points and active lava lakes. The drop from the rim to the floor was stepped by ledges that marked former levels of lava in the caldera. It is therefore possible that the Keanakakoi deposits were generated by deep-seated explosions (deeper than 500 m and perhaps as deep as 700 m) within Kilauea, and that the rim of the eruptive vent was several hundred meters below the rim of the caldera. Eruptive events that produced ejecta unable to clear the former caldera rim have been screened from the record of the eruption as seen in deposits on the modern caldera rim and beyond.

Reconstruction of the Keanakakoi ash eruption

The Keanakakoi ash eruption opened with explosive, steam-driven disruption of the oxidized and altered crust capping the lava surface, deep in the conduit (lithic-rich, accretionary lapilli-bearing fine ash, layer 0). Thereafter, actively vesiculating magma was supplied to the open vent, but subjected to further explosive fragmentation on encountering groundwater before ejection in steam-rich eruption plumes (layers 1, 2, 3, 4). Hundreds of explosions are recorded by the lower division clearly repeating a definite pattern (Fig. 9c: 1, 2, 3), such as (a) rising of the magma in the conduit in response to buildup of volatile pressure; (b) vesiculation and partial fragmentation of the magma; (c) mixing of the variably vesiculated fragments with water and/or steam at the level of the aquifer; (d) steam- and volatile-driven explosive eruption of the thoroughly fragmented, mostly juvenile ejecta; (e) deflation and subsidence of the remaining degassed magma below the site of interaction with water, resetting conditions favorable to (a). The vertical oscillation of the magma level may have been short, perhaps only a few metres, because the volume of material expelled by each separate explosion, preserved by individual beds or coarse + fine pairs of beds, was small. This phase appears to have been controlled by the magma volatile pressure, given apparently steady and balanced magma and water supplies. Two larger cycles are also evident in that layers 1 and 3 are overall coarser than 2 and 4, reflecting couplets of more vigorous followed by less vigorous explosion series perhaps related to subtle shifts in the magma:water mass ratio.

The first major departure from the opening phreatomagmatic activity followed a break (e1), during which considerable aeolian erosion and redeposition affected the fresh mantle of fallout ash. During the break, the degassed magma may have remained at much the same level as before, but it was prevented from mixing with groundwater because either (1) it was not fragmented, (2) the groundwater may have been temporarily exhausted by the earlier explosions, and/or (3) it was insulated by a stabilized jacket of steam.

Eventually a new batch of magma rose, vesiculated, and erupted free of interference by groundwater to form the scoria lapilli fall (layer 6). The isopach and isopleth maps (Figs. 6d and 7a) suggest the possibility that layer 6 emanated from a vent slightly displaced from the source area for preceding and following eruptions, a circumstance which would help to account for the markedly "dry" style of this explosion compared with the others. Isopachs of layer 7 (Fig. 6e) indicate eruption from the former source area. Layer 7 is rich in oxidized and altered ash, and may be derived from a crust that had developed above the stagnant lava in the main conduit during the e1 break. Fluvial gullies excavated into layer 7 (e2) record a second interruption of sufficient duration for rain storms to gather and break. Later, the groundwater reservoir recovered and the supply of fresh magma resumed, initiating a second series of phreatomagmatic explosions that produced more well-bedded vitric ash (layers 8, 9, 10; Fig. 9c: 1, 2, 3). These deposits are in most respects similar to layers 1 to 4, though somewhat richer in accretionary lapilli. Toward the end of this series, lava locally reached the surface via a route away from the main conduit in the caldera, bypassing the aquifer altogether.

On cessation of the phreatomagmatic explosions, the first of two main stages in the Keanakakoi ash eruption ended. There is good evidence for a pause (e3) during which aeolian erosion and reworking redistributed the ash, and at least the southwestern margins of the ash blanket were visited by Hawaiians, as recorded by

their footprints on an accretionary lapilli-bearing ash-fall bed in layer 9 (location 78, Fig. 10; see also Jaggar 1921). This wet ash later dried out and cracked before being covered by dunes drifting downwind during the e3 break. The magma subsided deeper into the conduit, removing support for the already weakened and fractured vent walls. A small number of discrete, powerful, steam-driven explosions registered the final events (phase 3) in the Keanakakoi ash eruption. Magma did not participate directly but was the heat source for steam production. The explosions ejected country rock and congealed, degassed lava, either as blocks or as pulverized and milled fine wet ash (upper division, Fig. 9d).

At least four major explosions were responsible for the upper division. Layer 11 may be the product of an initial, relatively weak ash plume eruption that was quickly overtaken by a more vigorous outburst of laterally directed base surges (layer 12a). Couplets comprising a lower block or lapilli fall bed overlain by dune-bedded surge deposits (e.g., layers 12b+12c; layers 14+15) are interpreted to record eruption column collapse events. Layer 13 is actually a composite of one block fall horizon sandwiched between upper and lower accretionary lapilli-bearing, fine, fallout ash beds. Some time after phase 3 ended, footprints were impressed upon one of the layer 13 accretionary lapilli-bearing, fine ash beds downwind of the caldera (locality 78), before being alternately concealed then revealed by shifting ash dunes, a process that continues today.

The spectacular activity responsible for Keanakakoi ash was eventually followed by fire fountaining and lava effusion from vents in the summit caldera, generating the golden pumice (Sharp et al. 1987).

Whereas the basal reticulite and the golden pumice indicate the presence of magma at Kilauea's summit, the intervening layers (0–16) record its retreat, evidently at a rate and to a depth ideally suited to explosive interaction with groundwater. A faster rate of retreat would allow magma to escape from the system before conditions conducive to magma-water interaction were established. At a slower rate, a steam jacket and selvedge of congealed lava could be maintained around the conduit, sealing the magma from direct encounters with water while it cooled.

Fig. 10. Fossil human footprints impressed into layer 9 (accretionary lapilli ash) at locality 78, Southwest Rift Zone about 9 km from Kilauea caldera rim. Note also the fossil dessication cracks; these formed when the wet fine ash dried out

The fatal explosion

The earliest written report of the 1790 eruption (Ellis 1827) based on the recollections of local Hawaiians described one explosion that resulted in the deaths of 80 people at an unspecified locality close to Kilauea. The more detailed account by Dibble (1843, p 51) refers to four main explosions, one on each of three successive nights, then the most violent during the next day. The last was fatal for all in the middle one of three parties of Keoua's warriors travelling separately along the same route from Kilauea southwest toward Kapapala. Some members of the forward party were also killed, while all in the rear party survived. Dibble does not specify the route followed or the precise positions of the three parties. Brigham (1909), Jaggar (1921), Finch (1947), and Swanson and Christiansen (1973) favor the north rim trail via Uwekahuna, whereas Douglas (1834), Hitchcock (1909), and S Powers (1916) favor the trail that passed south of the caldera.

The internal stratigraphy of the upper, lithic-rich division suggests that phase 3 involved about four or five explosive pulses. Although it is clear that each pulse was a complex combination of overlapping outbursts, the upper division stratigraphic record and the historic record are in excellent accord. The two earlier phases of the eruption did not feature in Hawaiian traditions probably because they were relatively mild and caused little inconvenience.

The fatal explosion may have been the second surge-generating event, recorded by block fall layer 14 and the immediately overlying base surge layer 15 (Fig. 2; Table 3). The dispersal of the block fall shows a strong southeastern bias, whereas the surges appear to have been directed to the southwest and to a lesser degree to the north of the caldera (Fig. 11). The positions of each of the three parties of warriors proposed by

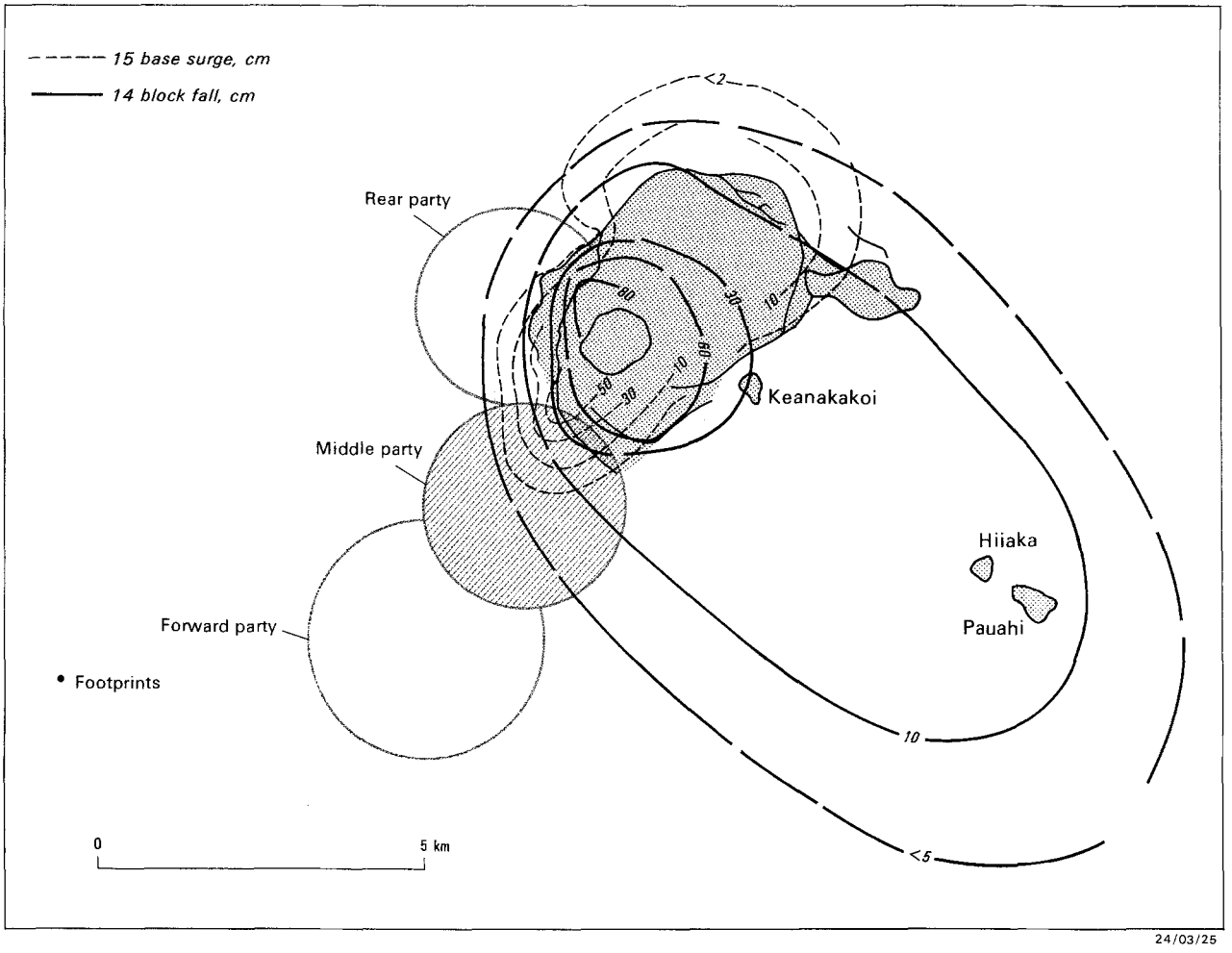

Fig. 11. Dispersal of layer 14 (block fall) and layer 15 (base surge) shown by isopachs in centimeters, compared with the positions of warrior parties proposed by Swanson and Christiansen (1973)

Swanson and Christiansen (1973, Fig. 1; Fig. 11) fit these dispersal patterns very well: the middle party would have been directly in the path of the southwest-directed surges, whereas the forward party was beyond the surge runout in this direction, and the rear party was safely located between the southwest- and north-directed surge lobes. All three probably experienced showers of lithic lapilli and ash because they were within, but on the margins of, the block fall (layer 14) dispersal. Of the three, the middle party was in the range of the coarsest and thickest layer-14 accumulation.

The warriors' camp was close to the caldera but evidently unaffected by the explosions of the first three nights. In particular, they escaped the base surges of layer 12 which would have scoured much of the western, southern, and southeastern margins of the caldera (Fig. 6g). The northwestern and northern section of the rim remained largely unaffected by earlier explosions, whereas sites near Keanakakoi crater, or elsewhere south of the caldera, would have been repeatedly showered by fallout ash and lapilli. The evidence presented here thus supports the north rim route as that travelled by the warriors, in agreement with Swanson and Christiansen (1973) and others.

Conclusions

The Keanakakoi Ash Member comprises three parts: reticulite layers at the base and the top are separated by well-bedded ash and lapilli (Keanakakoi ash). The reticulite layers record fire fountaining from vents within the summit caldera. The Keanakakoi ash eruption commenced within a long series of phreatomagmatic explosions separated into two phases by a period of repose during which the deposits were partially eroded. Phreatic explosions of the third phase followed after another pause. Most of Keanakakoi ash comprises fall deposits, accompanied by base surge deposits generated during the third phase.

Explosive hydrovolcanic eruptions from Kilauea caldera are rare. The special circumstance promoting such behavior over more typical lava effusion appears, in this case, to have been exceptionally deep withdrawal of magma in the summit conduit at a rate that was in delicate balance with the rate of degassing and of groundwater supply. Otherwise, neither the phreatomagmatic nor the phreatic activity would have occurred.

Any events leading to movement of magma from or

to the summit of Kilauea are potentially hazardous in their capacity to initiate explosive, phreatomagmatic or phreatic activity. An appropriate balance among the rates of magma withdrawal (or return), magma vesiculation and groundwater supply is evidently critical in promoting an explosive eruption. Phreatomagmatic phases involving vesiculating magma are likely to comprise long series of explosions, each similar in magnitude and effects, though displaying subtle variations in the course of the whole phase. Phreatic phases are expected when the magma reaches the deepest levels of the groundwater-saturated conduit during its final retreat (or first approach). These explosions are predicted to be diverse in style, effects, and duration and erratic in frequency.

Acknowledgements. This research was supported by NASA grant no. NAGW-541 (GPL Walker) and a Fulbright postdoctoral research fellowship (J McPhie). The cooperation of the Superintendent of the Hawaii Volcanoes National Park is gratefully acknowledged. KH Wohletz and RV Fisher are thanked for their thorough reviews.

References

Brigham WT (1909) The volcanoes of Kilauea and Mauna Loa on the island of Hawaii. BP Bishop Museum Memoir 2, Honolulu, pp 1–222

Carey S, Sparks RSJ (1986) Quantitative models of the fallout and dispersal of tephra from volcanic eruption columns. Bull Volcanol 48:109–125

Christiansen RL (1979) Explosive eruption of Kilauea Volcano in 1790 (abs). Hawaii Symposium on Intraplate Volcanism and Submarine Volcanism, Hilo, Hawaii, p 158

Decker RW, Christiansen RL (1984) Explosive eruptions of Kilauea Volcano, Hawaii. Explosive volcanism: inception, evolution, and hazards. Nat Acad Press, Washington DC, pp 122–132

Dibble S (1843) A history of the Sandwich Islands. Thos. G. Thrum, Honolulu (reprinted 1909)

Douglas D (1834) Extract from a private letter addressed to Captain Sabine, RA, FRS. J R Geogr Soc 4:333–344

Easton RM (1987) Stratigraphy of Kilauea Volcano. US Geol Surv Prof Pap 1350:243–260

Ellis W (1827) Journal of William Ellis, narrative of a tour of Hawaii or Owhyhee; with remarks on the history, traditions, manners, customs and language of the inhabitants of the Sandwich Islands. Reprinted 1979, Charles E Tuttle Company, Rutland, Vermont and Tokyo, Japan, pp 1–343

Finch RH (1947) Kilauea in 1790 and 1823. Volcano Lett 496:1–2

Heiken G, Wohletz KH (1985) Volcanic ash. Univ Calif Press, Berkeley

Hitchcock CH (1909) Hawaii and its volcanoes. Hawaiian Gazette Company, Honolulu, pp 1–314

Jaggar TA (1921) Fossil human footprints in Kau Desert. Hawaiian Volcano Observ Month Bull 9:114–118

Jaggar TA, Finch RH (1924) The explosive eruption of Kilauea in Hawaii. Am J Sci, Fifth Series, 8:353–374

Kokelaar P (1986) Magma-water interactions in subaqueous and emergent basaltic volcanism. Bull Volcanol 48:275–289

Malin MC, Dzurisin D, Sharp RP (1983) Stripping of Keanakakoi tephra on Kilauea Volcano, Hawaii. Geol Soc Am Bull 94:1148–1158

Powers HA (1948) A chronology of explosive eruptions of Kilauea. Pacific Science 2:278–292

Powers S (1916) Explosive ejectament of Kilauea. Am J Sci, Fourth Series 41:227–244

Sharp RP, Dzurisin D, Malin MC (1987) An early 19th century reticulite pumice from Kilauea Volcano. US Geol Surv Prof Pap 1350:395–404

Stearns HT, Clark WO (1930) Geology and water resources of the Kau district, Hawaii. US Geol Surv Water-Supply Pap 616, pp 1–194

Stone JB (1926) The products and structure of Kilauea. BP Bishop Museum Bulletin 33, Honolulu, pp 1–59

Swanson DA, Christiansen RL (1973) Tragic base surge in 1790 at Kilauea Volcano. Geology 1:83–86

Walker GPL (1984) Characteristics of dune-bedded pyroclastic surge bedsets. J Volcanol Geotherm Res 20:281–296

Walker GPL (1986) Koolau dike complex, Oahu: intensity and origin of a sheeted-dike complex high in a Hawaiian volcanic edifice. Geology 14:310–313

Walker GPL, Croasdale R (1972) Characteristics of some basaltic pyroclastics. Bull Volcanol 35:303–317

Wentworth CK (1938) Ash formations of the island Hawaii. Hawaiian Volcano Observatory Special Report 3, Hawaiian Volcano Research Association, Honolulu, pp 1–183

Wohletz KH (1983) Mechanisms of hydrovolcanic pyroclast formation: grain-size, scanning electron microscopy, and experimental studies. J Volcanol Geotherm Res 17:31–63

Wohletz KH (1986) Explosive magma-water interactions: thermodynamics, explosion mechanisms, and field studies. Bull Volcanol 48:245–264

Wright JV, Smith AL, Self S (1980) A working terminology of pyroclastic deposits. J Volcanol Geotherm Res 8:315–336

Zablocki CJ, Tilling RI, Peterson DW, Christiansen RL, Keller GV, Murray JC (1974) A deep research drill hole at the summit of an active volcano, Kilauea, Hawaii. Geophys Res Lett 1:323–326